Biochemical and Biophysical Research Communications 433 (2013) 477–483

Contents lists available at SciVerse ScienceDirect

Biochemical and Biophysical Research Communications

journal homepage: www.elsevier.com/locate/ybbrc

Cysteine accessibility during As^{3+} metalation of the α- and β-domains of recombinant human MT1a

Gordon W. Irvine [a], Kelly L. Summers [b], Martin J. Stillman [a,b,*]

[a] Department of Chemistry, The University of Western Ontario, London, Ontario, Canada N6A 5B7
[b] Department of Biology, The University of Western Ontario, London, Ontario, Canada N6A 5B7

ARTICLE INFO

Article history:
Received 25 February 2013
Available online 21 March 2013

Keywords:
Electrospray ionization mass spectrometry
Metallothionein
Metal induced folding
Arsenic binding
Cysteine modification
Molecular mechanics
Molecular dynamics

ABSTRACT

Metallothionein is a ubiquitous metal binding protein that plays an important role in metal ion homeostasis and redox chemistry within cells. Mammalian metallothioneins bind a wide variety of metals including the metalloid As^{3+} in two domains (β and α) connected by a short linker sequence. Three As^{3+} bind in each domain for a total of 6 As^{3+} per protein. In recombinant human metallothionein (rh-MT1a) each As^{3+} binds three cysteine residues to form $As_3Cys_9(CysSH)_2$-α-rhMT1a in the 11 Cys α-domain and As_3Cys_9-β-rhMT1a in the 9 Cys β-domain. This means that there should be 2 free cysteines in the α-domain but no free cysteines in the β-domain. By using benzoquinone, the number and relative accessibility of the free cysteinyl thiols during the metalation reactions were determined. The electrospray ionization mass spectrometry (ESI-MS) data confirmed that each As^{3+} binds using exactly 3 cysteine thiols and showed that there was a significant difference in the reactivity of the free cysteines during the metalation reaction. After a reaction with two molar equivalents of As^{3+} to form $As_2Cys_6(CysSH)_3$-αβ-rhMT1a, the remaining 3 Cys in the 9 Cys β-domain were far less reactive than those in the α-domain. Molecular dynamics calculations for the metalation reactions with As^{3+} measured by ESI-MS allowed an interpretation of the mass spectral data in terms of the relative location of the cysteine thiols that were not involved in As^{3+} coordination. Together, these data provide insight into the selection of a specific cysteinyl thiol by the incoming metals during the stepwise metalation of metallothioneins.

1. Introduction

Metallothionein (MT), first isolated in 1957 [1], is a ubiquitous metal binding protein that plays an important role in metal ion homeostasis and redox chemistry within cells [2]. It has also been implicated in cancer prevention and the inflammation response [3]. MT binds a wide variety of metals including Zn^{2+}, Cu^{+}, Cd^{2+} and the metalloid As^{3+}. The structure of the full protein includes two metal-binding domains: the β (9 cysteines) and α (11 cysteines) domains connected by a short linker sequence. The structure of the metalated protein is well defined and is based almost completely on the effects of metal coordination [4].

Divalent metals bind with a stoichiometry of M_4Cys_{11} (α) and M_3Cys_9 (β) for an overall stoichiometry of M_7Cys_{20} (αβ). Up to 3 As^{3+} can bind in each domain for a total of 6 per two domain protein [5]. The structure of As_6Cys_{20}-βα-rhMT was previously inferred as being triangular pyramidal based on $As(Cys)_3$ coordination because of the presence of the nonbonding pair on the As^{3+} [5]. Therefore, when fully saturated with As^{3+}, there would be two free cysteines in the α domain ($As_3Cys_9(CysSH)_2$), but no free cysteines in the β domain (As_3Cys_9). From the kinetics of the metalation reaction with As^{3+}, the α domain is known to exhibit higher binding constants than the β domain [6]. While the kinetic analysis provided a clear interpretation of the stepwise metalation, there are no published data to confirm that the stoichiometry is as shown above. Although the structure of MT is dominated by metal induced folding, the structure of apo-MT and partially metalated MT is largely unknown [7]. It is unclear as to what conformations the protein adopts as each metal binds in a stepwise fashion and how these intermediate conformations may affect subsequent metal binding events. Recently, we have reported that benzoquinone-thiol chemistry can be used to quantify the presence of free cysteine residues in MT [8]. The benzoquinone (Bq) covalently binds with the SH group of the cysteine and the extent of the reaction can be determined using ESI-MS.

The incoming Bq molecule will readily react with cysteines on the surface of the protein, but the reaction of Bq with interior residues is likely to require excess Bq. The same is true for the concentration of an incoming metal ion required to fully saturate all the possible metal binding sites. The structures of the metal-free and partially metalated species of MT will affect the rate at which the binding of subsequent metals occurs because of the accessibility of the free cysteinyl thiols required for metal coordination. Structures of these intermediates are almost impossible to obtain, so

* Corresponding author. Address: Department of Chemistry, Chemistry Building, The University of Western Ontario, London, Ontario, Canada N6A 5B7.
E-mail address: martin.stillman@uwo.ca (M.J. Stillman).

0006-291X/$ - see front matter © 2013 Elsevier Inc. All rights reserved.
http://dx.doi.org/10.1016/j.bbrc.2013.03.026

Bq can be used to probe the surface accessibility of the cysteinyl thiols. The structure of the partially metalated species is especially important because it dictates the extent to which any free thiol can be oxidized in the cell. The ease of oxidation of the thiols is important in determining the role metallothioneins might play in cellular redox chemistry [2].

The reaction of As^{3+} with different metallothioneins has been well documented [9,10]. The kinetic analysis of Ngu et al. provides detailed parameters that describe each stage of the metalation [10]. The slow rate of the As^{3+} metalation with the domain fragments of human MT1a was exploited in this work to isolate the individual species of As_n–MT (n = 1–3) formed with 1–3 equivalents of As^{3+}. We report the use of Bq to quantify the number and relative accessibility of the free cysteinyl thiols as the As^{3+} binding proceeds stepwise.

2. Materials and methods

The expression and purification methods have been previously reported in detail [11]. Briefly, the α- and β-domains (α-rhMT and β-rhMT, respectively) of human recombinant MT 1a were used in this study and have the following sequences: β-rhMT 1a MGKAAAACSC ATGGSCTCTG SCKCKECKCN SCKKAAAA and α-rhMT 1a GSMGKAAAAC CSCCPMSCAK CAQGCVCKGA SEKCSCCKKA AAA. The expression was carried out in *Escherichia coli* strain BL21(DE3) using a pET29a plasmid. The "1a" refers to the 1a isoform of human MT. The proteins contain no disulfide bonds or aromatic amino acids. An N-terminal S-tag with the sequence MKETAAAKFE RQHMDSPDLG TLVPRGS was used for the expression to aid in protein stability throughout the purification process. The S-tag was removed via a Thrombin CleanCleave™ kit (Sigma). To prevent cysteine oxidation, all solutions were argon saturated before use and thoroughly evacuated before storage. Protein samples were demetalated using Tris buffer, pH adjusted using HCl to 2.7 and centrifuged in an Amicon Ultra Centrifugal Filter Tube (Millipore) with a 3 kDa MW filter. The samples were then buffer exchanged with 10 mM ammonium formate (pH 3.5) to desalt and achieve the proper reaction pH for the metalation with arsenic.

Solutions of 150 mM parabenzoquinone (Bq; Fisher Scientific) were prepared in 100% methanol (Caledon Laboratory Chemicals) and diluted to 15 mM in deionized water. Solutions of 1.3 mM As^{3+} were prepared by dissolving As_2O_3 in concentrated HCl and diluting with deionized water. The pH of the solution was then adjusted to 3.5 using NH_4OH. All solutions were evacuated and saturated with argon before use.

Protein concentrations were determined by remetalation with Cd^{2+} and examination of the UV–visible absorption spectrum at 250 nm, which corresponds to the ligand-to-metal charge transfer transition of the Cd-thiolate bond ($\varepsilon_{\beta;250\ nm}$ = 36,000 M^{-1} cm^{-1} and $\varepsilon_{\alpha;250\ nm}$ = 45,000 M^{-1} cm^{-1}).

Mass spectra were collected on a microTOF II electrospray-ionization time-of-flight mass spectrometer (Bruker Daltonics, Canada) in the positive ion mode as previously described [8]. Spectra were constructed and deconvoluted using the Bruker Compass Data Analysis software package.

Molecular modeling calculations were carried out using Scigress Version 3.0.0 (Fujitsu Poland Ltd.). Modeling parameters and sequence information have also been previously described [8,12].

3. Results and discussion

Fig. 1A shows the ESI-MS data recorded for the metal free, apo-α-rhMT with mass 4081.8 Da. Arsenic metalation occurs over a long time scale with the 1–3 M equivalents added taking about an hour to reach equilibrium in α-rhMT and slightly longer in β-rhMT [6]. It was possible to monitor the reaction using ESI-MS to determine when each intermediate ($As_nCys_{(3n)}$ n = 1–3) species was most abundant and then introduce the Bq, effectively quenching the reaction. Fig. 1B shows the ESI-MS data after 1 h equilibration following the addition of 1 mole equivalent of As^{3+}. The data show that there are 3 species of α-rhMT present: apo-α-MT, As_1-α-rhMT and As_2-α-rhMT (in order of decreasing abundance). These data confirm the noncooperativity of the As^{3+} metalation reaction because very little As_3-α-MT forms. The free cysteines in these intermediate species were then modified by reaction with Bq. The addition of Bq quenched the metalation reaction as the modified cysteines were no longer able to participate in metal binding (Figs. 1 and 2). In this way, the reaction with Bq probes the availability of free cysteine residues at different points throughout the stepwise As^{3+} metalation.

An excess amount of Bq (40 mole equivalents) was added to the reaction vial and the ESI mass spectra were recorded. Fig. 1C shows ESI-MS data after the excess addition of Bq to the solution measured in Fig. 1B. All 11 cysteine residues of apo- α-rhMT were modified by binding 11 Bq resulting in a mass of 5258.9 Da. Similarly, As_1-α-rhMT had 8 cysteines modified for a final mass of 5008.7 Da, and As_2-α-MT had 5 cysteines modified for a mass of 4760.6 Da. There was a very small amount of the As_3-α-rhMT species present, the two free cysteines were modified by binding 2 Bq resulting in a mass of 4513.5 Da. The mass spectral data accounted for all the cysteines in each domain.

In a separate experiment, 3 mole equivalents of As^{3+} were added to apo-α-rhMT and the solution was equilibrated for 1 h. The spectrum in Fig. 1D shows that, when compared with the species in Fig. 1B, the abundance of the apo-α-rhMT and As_1-α-rhMT species decreased and the proportion of As_2-α-rhMT and As_3-α-rhMT increased, with As_3-α-rhMT being the most abundant as expected with the increased concentration of As^{3+}. In this case, a limiting amount of 2 mole equivalents of Bq were added to the solution after the spectrum in Fig. 1D was measured to probe the availability and accessibility of the free cysteines. The data in Fig. 1E illustrate the distribution of the free cysteines. The As_3-α-rhMT species can be seen without Bq modification and with 1 and 2 Bq bound. The abundances of the different Bq species detected for both As_2-α-rhMT and As_3-α-rhMT follow an approximately normal distribution. The mass spectrum for the complete modification of all free cysteines, achieved by adding a 10-fold excess of Bq, Fig. 1F, shows the presence of As_3-α-rhMT with 2 Bq and As_2-α-rhMT with 5 Bq (4513.4 and 4766.6 Da, respectively) as expected for the fully modified protein species.

The As^{3+} metalation and Bq reactions of apo-β-rhMT measured by ESI-MS are shown in Fig. 2. The apo-β-rhMT has a mass of 3752.6 Da (Fig. 2A). Because As_3-β-rhMT has no free cysteines, the metalation reaction was quenched after 1 h by addition of 2 mole equivalents of As^{3+} (Fig. 2B) to ensure that As_1- and As_2-β-rhMT were the dominant species and probe Cys accessibility. The mass spectrum shows that the most abundant species were As_2-β-rhMT (3896.1 Da) and As_1-β-rhMT (3824.1 Da) with no appreciable amount of apo-β-rhMT or As_3-β-rhMT. Addition of 10 mole equivalents of Bq resulted in the spectrum shown in Fig. 2C. Unexpectedly, the excess Bq did not react with all the free cysteines present. Significant fractions of unreacted As_1-β-rhMT and As_2-β-rhMT remained, as well as an approximately normal distribution of 1–3 Bq bound to As_2-ββ-rhMT and 1–4 Bq bound to As_1-β-rhMT (Fig. 2B). Not until 40 mole equivalents of Bq had been added did all 6 of the free cysteines in As_1-β-rhMT react (4465.2 Da). However, even under these harsh conditions not all of the free cysteines in As_2-β-rhMT reacted with Bq since there remained significant fraction of As_2-β-rhMT with only 1 or 2 Bq bound.

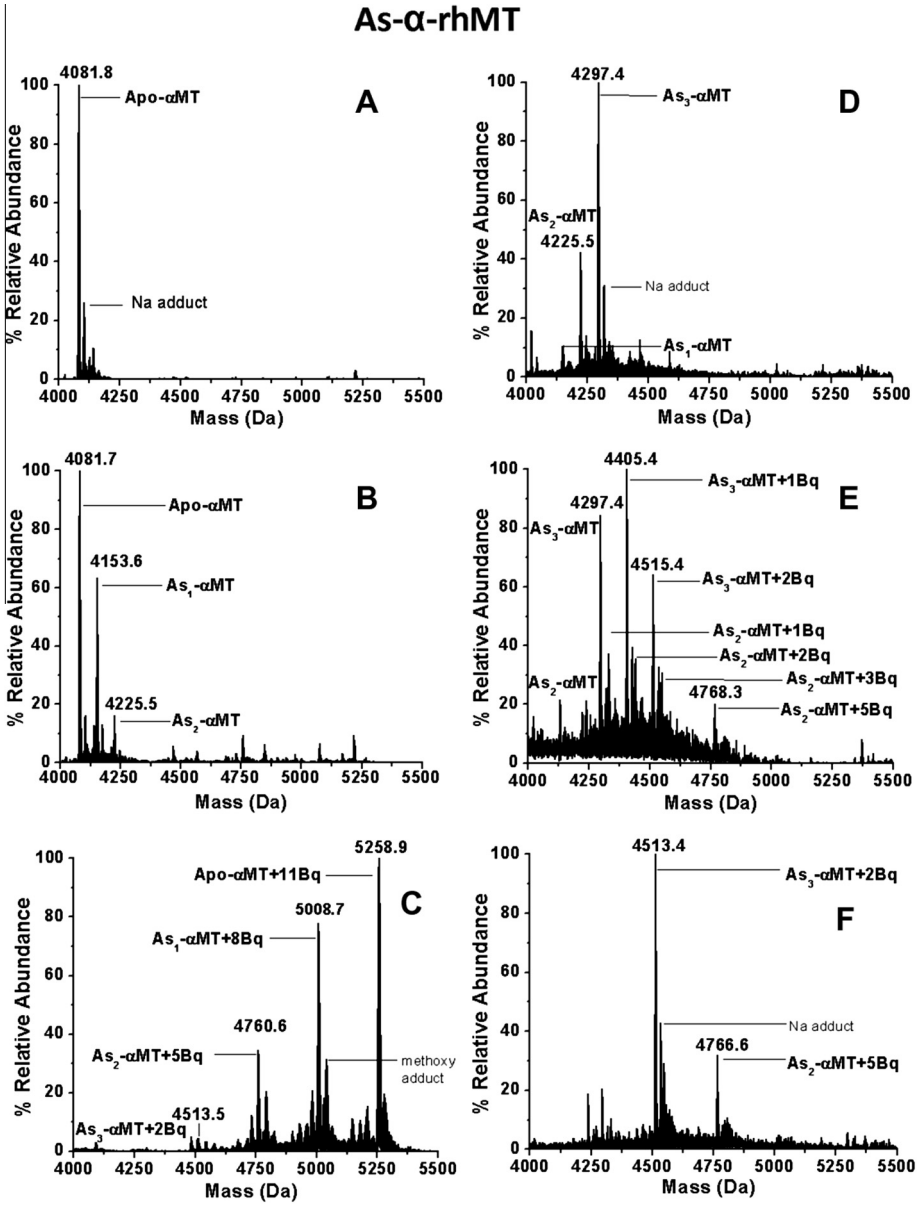

Fig. 1. ESI mass spectra of α-rhMT1a with increasing As^{3+} loading and cysteine modifications to form As_n-α-rhMT (n = 1–3). (A) Metal-free apo-α-rhMT. (B) After 1 h equilibration with 1 mole equivalent of As^{3+} added. (C) After 40 mole equivalents of Bq added to the solution in B. (D) After 1 h equilibration with 3 mole equivalents As^{3+} added to the apo-α-MT solution. (E) After 2 mole equivalents of Bq added to As_n-α-rhMT shown in D. (F) After 10 mole equivalents of Bq added to As_n-α-rhMT species shown in D.

While 40 mole equivalents of Bq resulted in complete modification of the free cysteines in As_n-α-rhMT (n = 0–3; Fig. 1B and C), there was only partial modification of the free cysteines in As_n-β-rhMT (n = 1–2; Fig. 2B and C). We believe this is a result of differences in accessibility of the cysteine residues between the two domains. The kinetic data clearly indicated that As^{3+} metalation was faster for the α- than for the β-domain. If the cysteines in partially metalated β-rhMT are buried inside the protein, then access will be sterically limited. The kinetic analysis of Ngu et al. showed that the rate at which the third As^{3+} bound to the β-domain of MT was much slower than that of the α-domain [6]. This may be because the overall protein structure of the intermediate As_2-β-rhMT shields the remaining cysteinyl thiols more than the structure of As_2-α-rhMT. Since a Bq molecule is larger than an As^{3+} ion, Bq binding would be more strongly affected by the steric hindrance around a cysteine.

3.1. Molecular models based on molecular dynamics calculations

A number of publications have reported molecular dynamics calculations of the Zn- and Cd–MTs [10,12–18]. The first reports showed that the models successfully reproduced the reported structures from X-ray diffraction and NMR studies. Indeed, the models predicted bond length similarities and coordination geometries that were later confirmed by use of XANES data and more exact calculations [18]. We have recently reported on the correlation between globular volume of α-, β-, and βα-rhMT and the charge states in the ESI-MS data [8]. The models reported by Rigby et al. showed that the apoprotein adopted a loose globular structure with the cysteinyl thiols near or on the surface [12,17]. Metalation always results in buried metal clusters inside the globular structure. One would expect that As_2-β-rhMT would readily react with 3 Bq. The data in Figs. 1 and 2 showed that both α- and β-rhMT

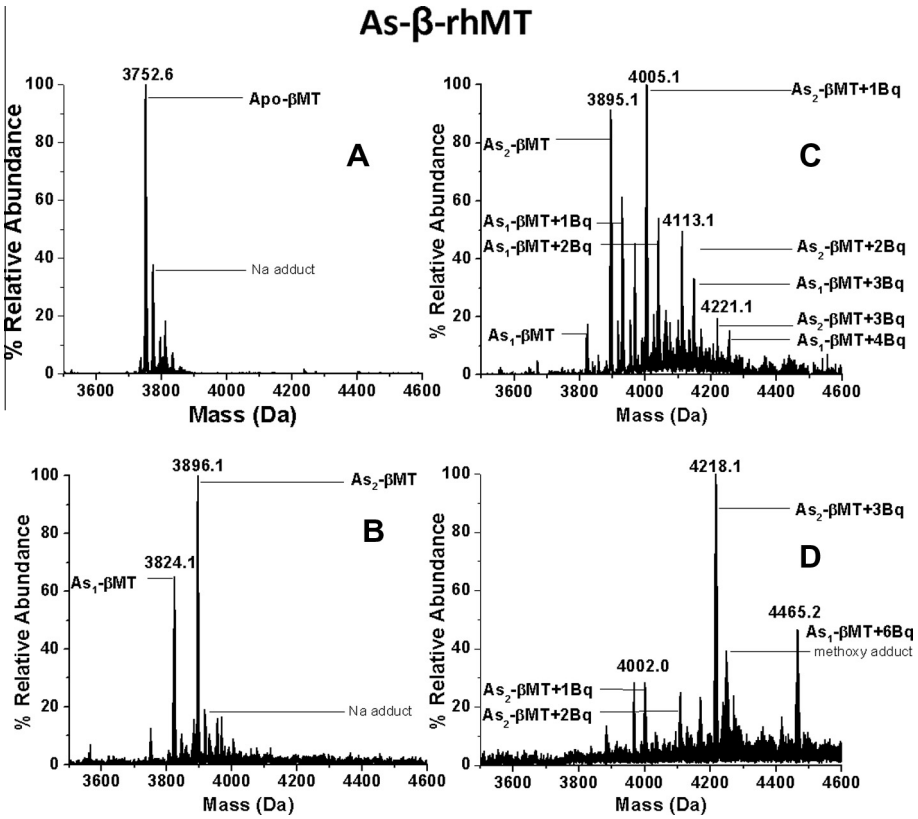

Fig. 2. ESI mass spectra of β-rhMT1a showing As^{3+} binding and cysteine modification with Bq to form As_n-β-rhMT (n = 1–2) using Bq. (A) Metal-free apo-β-rhMT. (B) After 2 mole equivalents of As^{3+} added to solution of apo-β-rhMT. (C) After 10 mole equivalents of Bq added to As_n-β-rhMT species shown in B. (D) After 40 mole equivalents of Bq added to As_n-β-rhMT species shown in B.

bound 3 As^{3+} only when the As^{3+} was added in excess. The ESI mass spectral data in Fig. 1 also showed that the free Cys in α-rhMT would react with Bq so that no free Cys were available. However, the data also showed that both the metalation with As^{3+} and the reactions with Bq were greatly impeded in β-rhMT since the formation of the fully modified As_2-Bq_3-β-rhMT required a 40-fold excess of Bq before each of the free Cys were modified (Fig. 2).

Fig. 3 shows the results of six molecular dynamics calculations carried out at a nominal 190 K with the dielectric set for water. The models show that modification with Bq results in very little change in the overall volume and structure of the proteins (Fig. 3). Both retain the compact form reported previously, indicating the importance of H-bonding between the residues [8,12,17].

3.2. Models for As-binding to apo-α-rhMT1a

Fig. 3(A–F) shows a series of models that represent As^{3+} metalation and Bq modifications for α-rhMT. Cys residues were chosen in sets of three for As^{3+} binding based on the report of Ngu et al., which suggested that the As^{3+} added sequentially from the C-terminus [6]. The kinetic analysis of Ngu et al. revealed a linear trend with respect to the order of the As^{3+} being added - with the exception of the first As^{3+}. The binding rate of the first As^{3+} bound was much slower than expected for both the α-domain and the full protein. Because the N-terminal Cys of the α-domain is constrained by the presence of the C-terminal β-domain in the full protein, it was concluded that the site of binding for As^{3+} would have to be the C-terminus. Bq was added to all free Cys for the As_1-, As_2- and As_3-species. Unlike the β-domain (9 Cys), the α-domain (11 Cys) has two free Cys when saturated with As^{3+}. The ESI mass spectral data described above confirm that the stoichiometry of 3 Cys per As^{3+} is maintained throughout the titration. The MD calculations show that the Bq are not only located on the outside of the structure, but also tend to be located adjacent to each other (highlighted in blue in Fig. 3). This might indicate aggregation of the hydrophobic Bq in the presence of the dielectric for water. Current spectroscopic experiments should allow us to determine if there is interaction between the Bq molecules when bound to the protein rather than when in dilute solution.

3.3. Models for As-binding to apo-β-rhMT1a

Similar to the models created for the α-domain, those constructed for the β-domain were based on the kinetic data of Ngu et al. and the first As^{3+} was assigned to the first three Cys at the C-terminus and Bq was then added to the remaining 6 free Cys [6].

The As_2-β-rhMT model was formed by selecting the second set of three Cys and adding 3 Bq to the remaining Cys, and finally, As_3-β-rhMT was formed by connecting the last three Cys to the third As^{3+}. In each case, the bound As^{3+} is located inside the structure surrounded by the peptide (as shown by the ribbon, Fig. 4). The Bq groups again migrate to the outside of the structure where one might consider the hydrophilic residues dominate. The bulk of the Bq clearly drives the orientation.

3.4. The special case of As2-β-rhMT

Fig. 2 shows the data for the addition of both As^{3+} and Bq to the β-domain fragment. As described above, the Bq did not readily react with the three free Cys of As_2-β-rhMT. This was unexpected as the reaction between Bq and thiols is normally fast and approximately stoichiometric. We calculated the structures for the

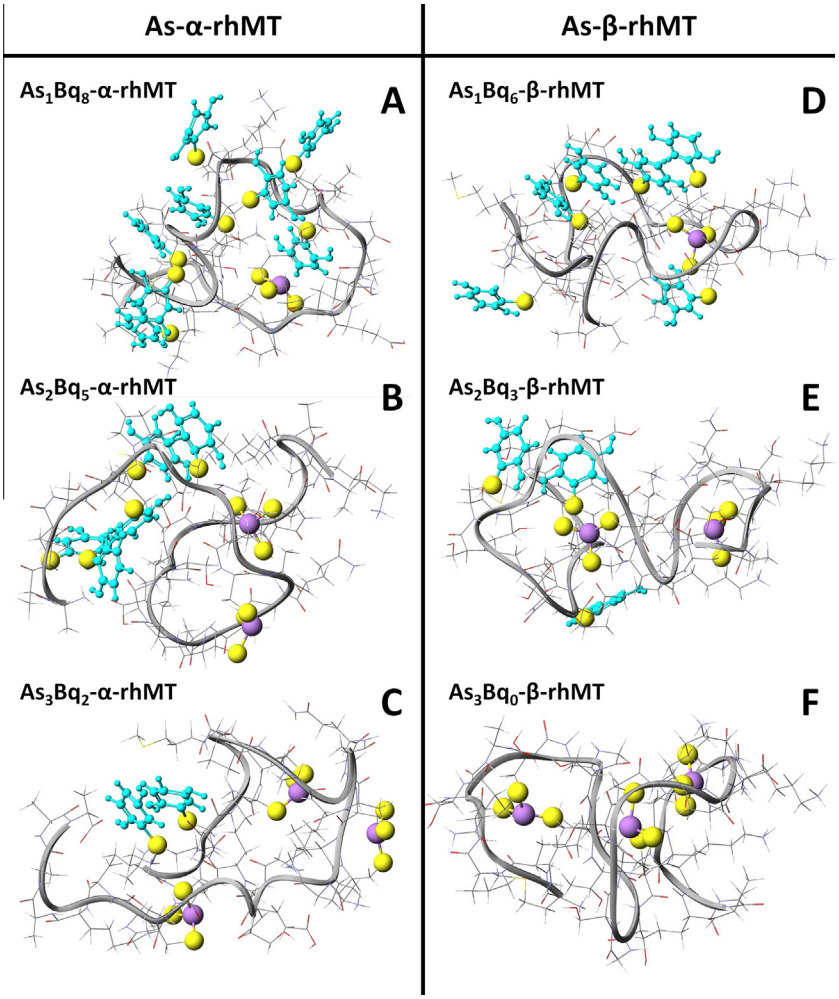

Fig. 3. Results of molecular dynamics (MD) calculations for As- and Bq-containing β-rhMT 1a (A–C) and β-rhMT 1a (D–F). Calculations were performed at 190 K over 2000 ps where all free cysteine are connected to Bq. Models are organized as follows: (A) As_1Bq_8-α-rhMT, (B) As_2Bq_5-α-rhMT, (C) As_3Bq_2-α-rhMT, (D) As_1Bq_6-β-rhMT, (E) As_2Bq_3-β-rhMT, and (F) As_3Bq_0-β-rhMT.

stepwise addition of Bq to As_2-β-rhMT (Fig. 4). There are two representations of each model: the ribbon, Cys thiols, Bq, and 2 As^{3+} are highlighted on the left, while the space-filling representations overlaid with the ribbon and the Bq are shown on the right. The Cys thiols are identified by the yellow spheres, the free thiols chosen for Bq binding are identified by arrows. Overall, the structures retain the globular properties reported previously [8]. The most exposed Cys were chosen each time for the Bq connection. We see that two Cys are accessible in the model of As_2-$(CysSH)_3$-β-rhMT (Fig. 4A), whereas the third Cys is buried and less accessible to incoming Bq. Similar to the MD calculations above, the β-domain model resulted in Bq aligning on the outside of the protein surface (Fig. 4B–D). The space-filling representation is overlaid with the ribbon and the Bq is again highlighted in blue (Right-hand column, Fig. 4). This view illustrates how the Bq lies in a crevice in the protein; the structure is dominated by the folding induced by the two As^{3+} bound to the 6 Cys.

The second Bq was connected to the second most exposed CysSH (arrow) and the model recalculated (Fig. 4C). Again, the Bq orient themselves in crevices on the surface. The last free Cys is still embedded in the protein and not readily accessible by the Bq. Connecting the third Bq and recalculating the model provides the last of the images in Fig. 4C. As with the α-rhMT modifications, it appears that the Bq molecules will associate if possible. In this case all three Bq's are located in crevices on the outer surface (Fig. 4C, right side).

3.5. Metalation of metallothioneins and interpretation of the mass spectral results using the models

When the mechanism for the metalation of a protein is studied, the chemical form and function of the metal binding site in the apo-protein must be considered. Metalation of metalloproteins (from apo- to holo-) may or may not result in major conformational or structural changes; often there are only minor changes. For metallothioneins, major structural changes are expected because there is little formal secondary structure in the metal-free apo-protein; metalation directs the secondary structure in the metalated form [12,17]. The ESI-MS data were expected to show systematic, complete modification of the free CysSH when excess Bq was added to solutions of partially metalated protein species with free cysteines. For the α-domain fragment this was observed. The mass spectral data confirmed that As^{3+} binds to MT using just three CysSH rather than the four used by Zn^{2+} and Cd^{2+}. However, the Bq did not readily bind to the free CysSH in the β-domain when there were three available in the As_2-β-rhMT species. The reactivity of the last 2 Bq molecules was so reduced that a large excess of Bq had to be used. The mass spectral data and the models suggest

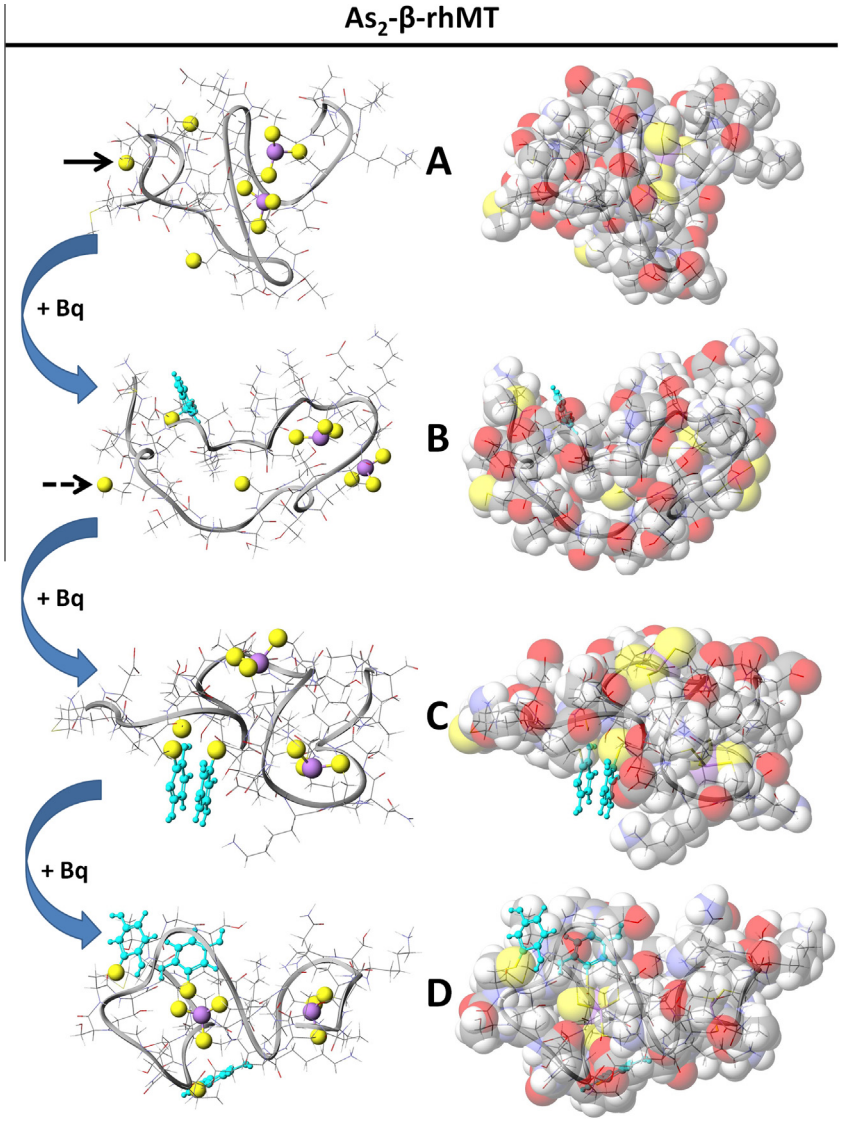

Fig. 4. Results of molecular dynamics (MD) calculations for As- and Bq-containing β-MT. Calculations were performed at 190 K over 2000 ps where the As_2Bq is modified in steps by Bq. Models are organized as follows: (A) As_2Bq_0-β-rhMT, (B) As_2Bq_1-β-rhMT, (C) As_2Bq_2-β-rhMT, and (D) As_2Bq_3-β-rhMT. At each step the structure was recalculated. There are two representations of each mode: (i) the ribbon structure highlighting the Cys thiols (yellow), Bq molecules (blue), and 2 As^{3+} (purple; left), and (ii) the space-filling representation with the backbone ribbon and the Bq (right). The arrows indicate the most exposed cysteine chosen for modification. (For interpretation of the references to color in this figure legend, the reader is referred to the web version of this article.)

that the cysteine residues in As_2-$(CysSH)_3$-β-rhMT are less accessible in the peptide fold than those in the α-domain and this may explain the much slower metalation rate reported in the stepwise metalation studies [6,10].

The data allow us to confirm unambiguously that the As^{3+} binds using exactly 3 thiols. The reaction of Bq with the cysteinyl thiols requires steric access to the free CysSH. The ESI-MS data reported here shows a difference in that access, which indicates that some of the cysteines are buried and less available for reaction. The molecular dynamics calculations allow an interpretation of the mass spectral data in terms of the relative location of the cysteine thiols that are not involved in As^{3+} coordination.

The data show that there is a difference in the relative binding affinities of the Bq for the Cys in the partially metalated α and β domains. Previously [8] it was reported that complete modification was achieved with only slight excess of Bq for the metal-free α-rhMT and β-rhMT fragments, indicating that the sequential modification of the peptide did not result in inaccessible Cys residues. The data here show that it is the metalation reaction that causes the Cys to become inaccessible and not the interference from modified residues on subsequent modifications.

Together, these data provide insight into the selection of a specific cysteinyl thiol by incoming metals during the stepwise metalation of metallothioneins. Furthermore, benzoquinone modification of cysteines will allow future determination of the coordination number for metals other than Zn^{2+} and Cd^{2+} where the coordination with the Cys thiol ligands is not well defined (for example Cu^{+}).

We conclude that the use of the Bq as a modifier provided not only a quantitative measure of free cysteine but also a means of probing the accessibility and hence the relative reactivity of the free cysteines.

Acknowledgments

We thank NSERC of Canada for financial support through Discovery and RTI Grants, and the Academic Development Fund at the University of Western Ontario for an equipment grant. We

wish to thank Mr Doug Hairsine for assistance with the mass spectrometry measurements, Dr. Maria Salgado Banegas for helpful suggestions and Mr. Michael Dryden for preliminary experiments.

References

[1] M. Margoshes, B.L. Vallee, A cadmium protein from equine kidney cortex, J. Am. Chem. Soc. 79 (1957) 4813.
[2] N. Chiaverini, M. De Ley, Protective effect of metallothionein on oxidative stress-induced DNA damage, Free Radical Res. 44 (2010) 605–613.
[3] T. Fukada, S. Yamasaki, K. Nishida, M. Murakami, T. Hirano, Zinc homeostasis and signaling in health and diseases, J. Biol. Inorg. Chem. 16 (2011) 1123–1134.
[4] J. Domenech, G. Mir, G. Huguet, M. Capdevila, M. Molinas, S. Atrian, Plant metallothionein domains: functional insight into physiological metal binding and protein folding, Biochimie 2006 (2006) 583–593.
[5] G. Jiang, Z. Gong, X.-F. Li, W.R. Cullen, X.C. Le, Interaction of trivalent arsenicals with metallothionein, Chem. Res. Toxicol. 16 (2003) 873–880.
[6] T.T. Ngu, A. Easton, M.J. Stillman, Kinetic analysis of Arsenic−Metalation of human metallothionein: significance of the two-domain structure, J. Am. Chem. Soc. 130 (2008) 17016–17028.
[7] J. Ejnik, J. Robinson, J. Zhu, H. Forsterling, C.F. Shaw III, D.H. Petering, Folding pathway of apo-metallothionein induced by Zn^{2+}, Cd^{2+} and Co^{2+}, J. Inorg. Biochem. 88 (2002) 144–152.
[8] K.L. Summers, A.K. Mahrok, M.D.M. Dryden, M.J. Stillman, Structural properties of metal-free apometallothioneins, Biochem. Biophys. Res. Commun. 425 (2012) 485–492.
[9] T.T. Ngu, J.A. Lee, M.K. Rushton, M.J. Stillman, Arsenic metalation of seaweed fucus vesiculosus metallothionein: the importance of the interdomain linker in metallothionein, Biochemistry 48 (2009) 8806–8816.
[10] T.T. Ngu, M.J. Stillman, Arsenic binding to human metallothionein, J. Am. Chem. Soc. 128 (2006) 12473–12483.
[11] J. Chan, Z. Huang, I. Watt, P. Kille, M.J. Stillman, Characterization of the conformational changes in recombinant human metallothioneins using ESI-MS and molecular modeling, Can. J. Chem. 85 (2007) 898–912.
[12] K.E. Rigby, M.J. Stillman, Structural studies of metal-free metallothionein, Biochem. Biophys. Res. Commun. 325 (2004) 1271–1278.
[13] D.A. Fowle, M.J. Stillman, Comparison of the structures of the metal-thiolate binding site in Zn(II)-, Cd(II)-, and Hg(II)-metallothioneins using molecular modeling techniques, J. Biomol. Struct. Dyn. 14 (1997) 393–406.
[14] A. Presta, D.A. Fowle, M.J. Stillman, Structural model of rabbit liver copper metallothionein, J. Chem. Soc., Dalton Trans. 49 (1997) 977–984.
[15] K.E.R. Duncan, M.J. Stillman, Metal-dependent protein folding: Metallation of metallothionein, J. Inorg. Biochem. 100 (2006) 2101–2107.
[16] M.E. Merrifield, J. Chaseley, P. Kille, M.J. Stillman, Determination of the Cd/S cluster stoichiometry in fucus vesiculosus metallothionein, Chem. Res. Toxicol. 19 (2006) 365–375.
[17] K.E. Rigby, J. Chan, J. Mackie, M.J. Stillman, Molecular dynamics study on the folding and metallation of the individual domains of metallothionein, Proteins 62 (2006) 159–172.
[18] J. Chan, M.E. Merrifield, A.V. Soldatov, M.J. Stillman, XAFS spectral analysis of the cadmium coordination geometry in cadmium thiolate clusters in metallothionein, Inorg. Chem. 44 (2005) 4923–4933.